Characterization of Na,K-ATPase and H,K-ATPase Enzymes with Glycosylation-Deficient β-Subunit Variants by Voltage-Clamp Fluorometry in *Xenopus* Oocytes[†]

Katharina L. Dürr,*[,‡] Neslihan N. Tavraz,[‡] Dirk Zimmermann,[§] Ernst Bamberg,[§,||] and Thomas Friedrich[‡]

Max Volmer Laboratory for Biophysical Chemistry, Institute of Chemistry, Technical University of Berlin, Secr. PC 14, Strasse des 17. Juni 135, D-10623 Berlin, Germany, Department of Biophysical Chemistry, Max Planck Institute of Biophysics, Max-von-Laue-Strasse 3, D-60438 Frankfurt/Main, Germany, and Chemical and Pharmaceutical Sciences Department, Johann Wolfgang Goethe University Frankfurt, Max-von-Laue-Strasse 1, 7-9, D-60439 Frankfurt/Main, Germany

Received January 17, 2008; Revised Manuscript Received February 20, 2008

ABSTRACT: The role of N-linked glycosylation of β-subunits in the functional properties of the oligomeric P-type ATPases Na,K- and H,K-ATPase has been examined by expressing glycosylation-deficient Asn-to-Gln β-variants in *Xenopus* oocytes. For both ATPases, the absence of the huge N-linked oligosaccharide moiety on the β-subunit does not affect α/β coassembly, plasma membrane delivery or functional activity of the holoenzyme. Whereas this is in line with several previous glycosylation studies on Na,K-ATPase, this is the first report showing that the cell surface delivery and enzymatic activity of the gastric H,K-ATPase is unaffected by the lack of N-linked glycosylation. Sulfhydryl-specific labeling of introduced cysteine reporter sites with the environmentally sensitive fluorophore tetramethylrhodamine-6-maleimide (TMRM) upon expression in *Xenopus* oocytes enabled us to further investigate potential effects of the N-glycans on more subtle enzymatic properties, like the distribution between E_1P/E_2P states of the catalytic cycle and the kinetics of the E_1P/E_2P conformational transition under presteady state conditions. For both Na,K-ATPase and H,K-ATPase, we observed differences in neither the voltage-dependent E_1P/E_2P ratio nor the kinetics of the E_1P/E_2P transition between holoenzymes comprising glycosylated and glycosylation-deficient β-subunits. We conclude that the N-linked glycans on these essential accessory subunits of oligomeric P-type ATPases are dispensable for proper folding, membrane stabilization of the α-subunit and transport function itself. Glycosylation is rather important for other cellular functions not relevant in the oocyte expression system, such as intercellular interactions or basolateral versus apical targeting in polarized cells, as demonstrated in other expression systems.

The ubiquitously occurring Na,K-ATPase and the closely related gastric H,K-ATPase, which is uniquely present in the highly specialized parietal cells of the stomach, are members of the P-type ATPase family comprising more than 200 identified members (*1*). Only Na,K- and H,K-ATPase isoenzymes and the bacterial Kdp-ATPase are oligomeric; Na,K- and H,K- ATPase require one (*2, 3*), the Kdp-ATPase two (*4*) associated subunits in addition to their catalytically active α-subunits for enzymatic activity. In contrast to the α-subunits of Na,K- and H,K-ATPase, which share about 60% sequence identity, the highest one observed in the whole ATPase family (*5*), the three Na,K β-subunit isoforms and the H,K β-subunits from different species exhibit only 20–30% overall sequence identity. A common feature, however, is the presence of several conserved N-glycosylation sites on the C-terminal extracellular domain (illustrated in Figure 1), resulting in a substantial increase of the mature subunits' molecular weight. This increase ranges from at least 80% for the Na,K-ATPase β_1-subunit, having only three N-linked glycosylation sites, up to more than 100% for the Na,K-ATPase β_2-subunit with 4 to 9, or the H,K-ATPase β-subunit possessing 6 to 7 glycosylation sites. Although studied in various expression systems, questions regarding the functional significance of these huge carbohydrate moieties have not been completely settled yet. Whereas removal of N-linked glycosylation on H,K-ATPase β-subunits has dramatic consequences in terms of α/β coassembly (*6*), plasma membrane delivery (*6, 7*) and catalytic activity (*6, 8*) of the holoenzyme, no such effects have been observed for the deglycosylated Na,K-ATPase (*9–13*).

However, the N-linked carbohydrates on the Na,K-ATPase β-subunit are crucial for some lectin-like properties (*14*), including a role in cell−cell adhesion of epithelial cells (*15*), neuronal interactions of β_2/AMOG[1] expressing glial cells (*16*) and isoform-specific basolateral versus apical targeting in

[†] This work was supported by the Max-Planck-Gesellschaft zur Förderung der Wissenschaften and a grant from the Deutsche Forschungsgemeinschaft (SFB 472).

* To whom correspondence should be addressed: Max-Volmer-Laboratory for Biophysical Chemistry, Institute of Chemistry, Secr. PC-14, Technical University of Berlin, Strasse des 17. Juni 135, D-10623 Berlin. Phone: +49-30-31423511. Fax: +49-30-31478600. E-mail: Katharina.Duerr@TU-Berlin.DE.

[‡] Technical University of Berlin.

[§] Max Planck Institute of Biophysics.

[||] Johann Wolfgang Goethe University Frankfurt.

[1] Abbreviations: AMOG, adhesion molecule on glial cells; VCF, voltage-clamp fluorometry; TMRM, tetramethylrhodamine-6-maleimide.

10.1021/bi800092k CCC: $40.75
Published on Web 03/15/2008

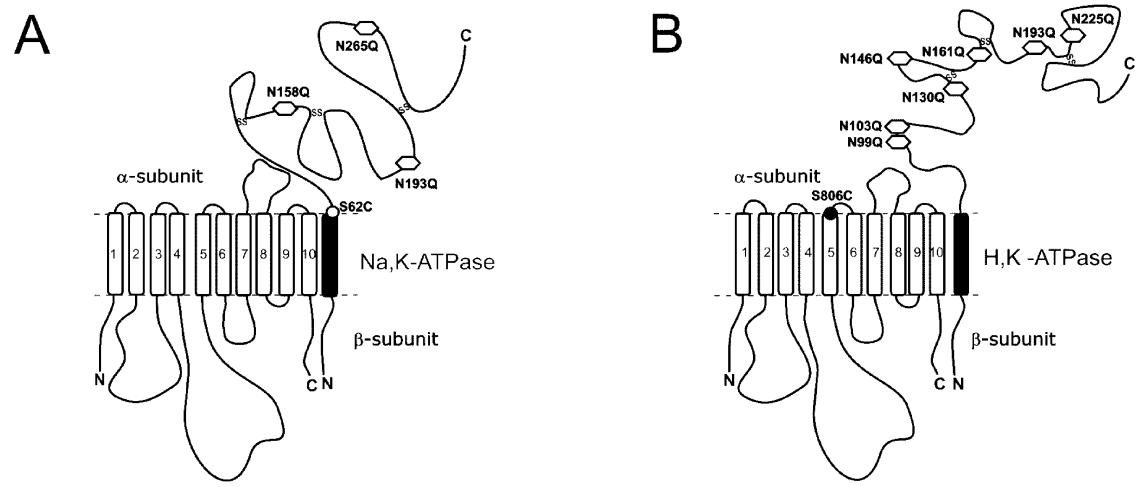

FIGURE 1: N-Glycosylation sites and mutations for site-specific labeling of Na,K- and H,K-ATPase. (A) The reporter site Ser-62C (open circle) and the three mutated N-glycosylation sites (hexagons) on the Na,K-ATPase β-subunit (black) are shown. (B) The reporter site Ser-806C (closed circle) on the H,K-ATPase α-subunit (white) and the seven mutated N-glycosylation sites (hexagons) on the H,K-ATPase β-subunit (black) are shown. "S−S" denotes disulfide bridges, and amino and carboxy termini are indicated as N and C, respectively.

various polarized cells (*17–19*). Likewise, the N-glycans on the H,K-ATPase have been shown to be essential for apical targeting (*19, 20*), protection from proteolytic digestion (*21, 22*) and acidic denaturation (*23*).

Thus, to differentiate between mainly *in situ* relevant secondary effects and primary effects on the functional properties of the enzyme itself, we aimed to investigate the as yet unknown functional significance of N-linked glycans for the H,K-ATPase using the *Xenopus* oocyte expression system. Another aspect of N-linked glycosylation, which has not been examined in P-type ATPases so far, is whether the presence of the huge oligosaccharide moiety has any effect on the kinetics of the E_1P/E_2P conformational transition or the distribution between E_1P/E_2P states of the catalytic cycle. Remarkably, the magnitude of fluorescence intensity changes upon K^+ addition to FITC-labeled, purified Na,K-ATPase was about 50% larger compared to the fully glycosylated enzyme, when N-linked oligosaccharides had been removed by a combined neuraminidase/endo-F treatment of the holoenzyme (*11*). This observation possibly reflects a shift in the enzymes' distribution between E_1/E_2 states. Regarding the substantial effect of N-linked sugars on the molecular weight of the holoenzyme, such a shift could arise from a kinetic effect on some particular steps in the catalytic cycle, which may in turn lead to changes in the apparent cation affinities.

To test this hypothesis, we utilized the technique of voltage-clamp fluorometry, which is the only available technique that allows presteady state kinetic investigations of electroneutrally operating ion transporters like the gastric H,K-ATPase in intact cells. This enabled us to directly monitor the voltage-dependent distribution of fluorescence-labeled H,K- or Na,K-ATPases between E_1P/E_2P states of the catalytic cycle in a time-resolved fashion.

EXPERIMENTAL PROCEDURES

Molecular Biology. The cDNAs of the sheep Na,K-ATPase β_1-subunit, rat H,K-ATPase β-subunit, rat H,K-ATPase α-subunit and a modified form of the sheep Na,K-ATPase α_1-subunit without extracellularly exposed cysteine residues (containing mutations C911S and C964A (*24*)) and with reduced ouabain sensitivity in the millimolar range (achieved by the mutations Q111R and N122D (*25*)) were subcloned into vector pTLN (*26*), as described (*27, 28*). The reduced ouabain sensitivity of the latter construct allows selective inhibition of the endogenous *Xenopus* Na,K-ATPase and was therefore used for all coexpression studies with β_1-constructs. Furthermore, to exclude any background signals in voltage-clamp fluorometric studies, which could possibly arise from Na,K-ATPase enzymes assembled from heterologously expressed α-subunits and endogenous β-subunits, we utilized the β_1-subunit sequence variant S62C for mutagenesis. The introduced cysteine is close to the transmembrane/extracellular interface (illustrated in Figure 1A) and has been shown to give rise to voltage-dependent fluorescence changes upon site-directed fluorescence labeling with TMRM without impairing enzyme function (*27*). To enable voltage-clamp fluorometry on gastric H,K-ATPase β-variants, we coexpressed a modified H,K-ATPase α-subunit with a single cysteine replacement S806C in the M5/M6 extracellular loop (see Figure 1B), which is homologous to the N790C mutation in the M5/M6 loop of the Na,K-ATPase α-subunit (*28*) and thus also suited for environmentally sensitive TMRM-labeling (*29*). Rubidium uptake measurements confirmed that the S806C mutation did not affect the H,K-ATPase's transport properties (see Supporting Information). Additional Asn-to-Gln mutations were introduced in all N-glycosylation sites present in the Na,K-ATPase β_1-ectodomain (N158Q, N193Q, N265Q, Figure 1A) or H,K-ATPase β-ectodomain (N99Q, N103Q, N130Q, N146Q, N161Q, N193Q, N225Q, Figure 1B) using the Quikchange Multi Site-Directed Mutagenesis Kit (Stratagene) and verified by DNA sequencing. The glycosylation-deficient Na,K-ATPase β_1-subunit and H,K-ATPase β-subunit constructs are termed NaKβgd (or NaKβS62Cgd) and HKβgd, respectively.

Oocyte Preparation and cRNA Injection. Xenopus oocytes were obtained by collagenase treatment after partial ovarectomy from *Xenopus laevis* females. cRNAs were prepared using the SP6 mMessage mMachine Kit (Ambion, Austin, TX). A 50 nL aliquot containing 20–25 ng of Na,K-ATPase and 1.5–2.5 ng of Na,K-ATPase β-subunit cRNA (or 20–25 ng H,K-ATPase α-subunit cRNA and 5 ng of H,K-ATPase

β-subunit) was injected into each cell. After injection, oocytes were kept in ORI buffer (110 mM NaCl, 5 mM KCl, 2 mM $CaCl_2$, 5 mM HEPES, pH 7.4) containing 50 mg/L gentamycin at 18 °C for 3 to 5 days for the Na,K-ATPase and for 2 days for the H,K-ATPase, respectively .

Isolation of Plasma Membranes from Xenopus laevis Oocytes. The isolation of plasma membranes was carried out according to Kamsteeg and Deen (*30*) with some modifications. After removal of their follicular cell layer, 8–12 oocytes were rotated in 1% colloidal silica (Ludox Cl, Sigma-Aldrich) in MES buffered saline for silica (MBSS; 20 mM MES, 80 mM NaCl, pH 6.0) for 30 min at 4 °C. After washing three times in MBSS, the oocytes were rotated at 4 °C in 0.1% poly(acrylic acid) (Sigma-Aldrich) in MBSS for 30 min and washed three times in Modified Barth's Solution (MBS; 0.33 mM $Ca(NO_3)_2$, 0.41 mM $CaCl_2$, 88 mM NaCl, 1 mM KCl, 2.4 mM $NaHCO_3$, 0.82 mM $MgSO_4$, 10 mM HEPES, pH 7.5).

Subsequently, oocytes were homogenized in 1.5 mL of buffer HbA (20 mM TRIS, 5 mM $MgCl_2$, 5 mM NaH_2PO_4, 1 mM EDTA, 80 mM sucrose, pH 7.4) containing protease inhibitor (Complete; Roche Mol. Biochem., Mannheim, Germany) and centrifuged for 30 s at 10 g at 4 °C, after which 1.3 mL of the sample supernatant was removed (to be saved for subsequent preparation of total membranes, see below) and 1 mL of HbA was added to the silica beads. This centrifugation and exchange of HbA was repeated four times, but centrifugation changed from twice at 10 g via once at 20 g to once at 40 g. After the last centrifugation step, HbA was removed and plasma membranes were spun down for 30 min at 16,000 g at 4 °C and resuspended in Laemmli buffer (*31*) (4 μL/oocyte).

Preparation of Total Membranes from Xenopus laevis Oocytes. To remove yolk platelets, the supernatant from homogenized oocytes in HbA containing protease inhibitor (see above) was centrifuged once for 3 min at 2,000 g at 4 °C, and the pellet discarded. Total membranes in the supernatant were spun down for 30 min at 16,000 g at 4 °C and resuspended in 4 μL/oocyte of Laemmli buffer (*31*).

Immunoblotting. Protein samples equivalent to 2 oocytes were separated on 12% SDS−polyacrylamide gels and blotted on nitrocellulose membranes (Roth). The α- and β-subunits of the sheep Na,K-ATPase were detected with the polyclonal anti-Na,K α-antibody C356-M09 (*32*) and the monoclonal anti-Na,K β-antibody M17-P5-F11 (*33*). The α- and β-subunits of the rat gastric H,K-ATPase were detected with the polyclonal anti-H,K α-antibody HK12.18 (*3*) (Merck) and the monoclonal anti-H,K β-antibody 2G11 (*34*) (Acris Antibodies), respectively. Subsequently, blots were incubated with appropriate HRP-conjugated secondary antibodies (Dako) and proteins were visualized by using an enhanced chemiluminescence kit (Roche Mol. Biochem., Mannheim, Germany).

Rb^+ Uptake Assay Using Atomic Absorption Spectrometry. Two days after injection, noninjected control oocytes and H,K-ATPase-expressing oocytes were preincubated for 15 min in a Rb^+ and K^+-free solution (90 mM TMACl, 20 mM TEACl, 5 mM $BaCl_2$, 5 mM $NiCl_2$, 10 mM HEPES, pH 7.4) containing 100 μM ouabain to ensure inhibition of the endogenous Na,K-ATPase and then incubated for 15 min in Rb^+-flux-buffer (5 mM RbCl, 85 mM TMACl, 20 mM TEACl, 5 mM $BaCl_2$, 5 mM $NiCl_2$, 10 mM MES, pH 5.5, 100 μM ouabain). After 3 washing steps in Rb^+-free washing-buffer (90 mM TMACl, 20 mM TEACl, 5 mM $BaCl_2$, 5 mM $NiCl_2$, 10 mM MES, pH 5.5) and one wash in water, each individual oocyte was homogenized in 1 mL of Millipore water.

To determine the apparent constant $K_{0.5}$ for half-maximal activation of the H,K-ATPase by rubidium, the sum [TMACl] plus [RbCl] in the Rb^+-flux buffer was kept constant at 90 mM, e.g. 1 mM RbCl + 89 mM TMACl. After subtraction of the mean of Rb^+ uptake into control oocytes from the same batch at a given RbCl concentration, the data was fitted to a Michaelis–Menten type function: $v = v_{max} \cdot [S] / (K_{0.5} + [S])$ Oocyte homogenizates were analyzed by atomic absorption spectroscopy using an AAnalyst800™ spectrometer (Perkin-Elmer, Waltham, MA). From oocyte homogenates (typically 1 mL) samples of 20 μL were automatically transferred into a transversely heated graphite furnace, subjected to a temperature protocol according to manufacturer's procedures (conditions available on request), and absorption was measured at 780 nm using a Rb hollow cathode lamp (Photron, Melbourne, Australia). After Zeeman-background correction, Rb^+ contents were calculated by comparison with standard calibration curves (measured between 0 and 50 μg/L rubidium). The detection limit (characteristic mass) of Rb^+ was ∼10 pg.

Oocyte Pretreatment, Fluorescence Labeling and Experimental Solutions. Prior to functional studies on Na,K-ATPase expressing oocytes, cells were first incubated for 45 min in Na^+-loading buffer (110 mM NaCl, 2.5 mM Na-citrate, 5 mM MOPS, 5 mM TRIS, pH 7.4), then for 15 min in postloading-buffer (100 mM NaCl, 1 mM $CaCl_2$, 5 mM $BaCl_2$, 5 mM $NiCl_2$, 5 mM MOPS/TRIS, pH 7.4) (*35*) to elevate the intracellular Na^+ concentration. For voltage-clamp fluorometry, site-specific labeling was achieved by incubating oocytes in postloading-buffer containing 5 μM tetramethylrhodamine-6-maleimide (TMRM, Molecular Probes, stock solution 5 mM in DMSO) for 5 min at room temperature in the dark, followed by extensive washes in dye-free postloading-buffer. Measurements under high extracellular Na^+/K^+-free conditions were carried out in Na^+-test-solution (100 mM NaCl, 5 mM $BaCl_2$, 5 mM $NiCl_2$, 5 mM MOPS/TRIS, pH 7.4, 10 μM ouabain). Stationary currents of the Na,K-ATPase were measured upon a solution exchange from 0 mM to 10 mM K^+ (10 mM KCl, 90 mM NaCl, 5 mM $BaCl_2$, 5 mM $NiCl_2$, 5 mM MOPS/TRIS, pH 7.4, 10 μM ouabain). The sheep Na,K-ATPase could be inhibited by 10 mM ouabain, the rat gastric H,K-ATPase by 10 μM SCH28080 (Sigma-Aldrich) or 30 μM omeprazole (Biotrend, Zürich, Switzerland).

Voltage-Clamp Fluorometry. An oocyte perfusion chamber was mounted in an Axioskop 2FS epifluorescence microscope (Carl Zeiss, Göttingen, Germany) equipped with a 40× water immersion objective (numerical aperture = 0.8). Currents were measured using a two-electrode voltage-clamp amplifier (Turbotec 05, npi, Tamm, Germany). Fluorescence was excited with a 100 W tungsten lamp using filters 535DF50 (excitation), 565 EFLP (emission) and 570DRLP (dichroic, all Omega Optical, Brattleboro, VT). Fluorescence was measured with a PIN-022A photodiode (UDT, Torrence, CA) mounted to the microscope camera port. Photocurrents were amplified by a low noise current amplifier DLPCA-200 (FEMTO, Berlin, Germany). Fluorescence and currents

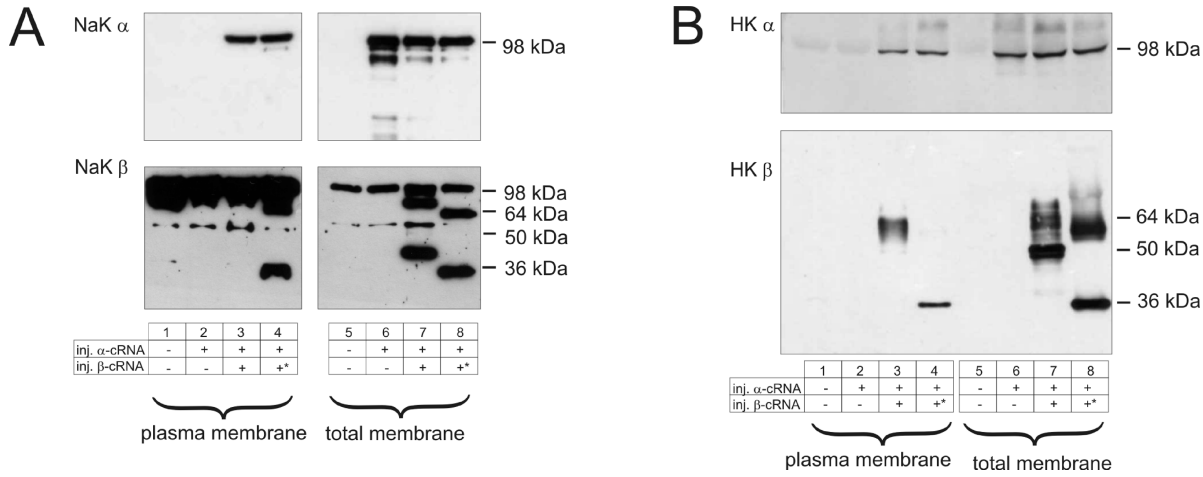

FIGURE 2: Western blot analysis of plasma membrane and total membrane fractions from Na,K- and H,K-ATPase-expressing oocytes. (A) Plasma membrane and total membrane fractions from oocytes injected with cRNAs for: NaKα only (lanes 2 and 6), NaKα + NaKβS62C (lanes 3 and 7), or NaKα + NaKβS62Cgd (lanes 4 and 8, see asterisks in the injection scheme), or from uninjected oocytes (lanes 1 and 5). Detection used Na,Kα-specific antibody C356-M09 (upper panel) or Na,Kβ-specific antibody M17-P5-F11 (lower panel). (B) Plasma membrane and total membrane fractions from oocytes injected with cRNAs: for HKαS806C only (lanes 2 and 6), HKαS806C + HKβwt (lanes 3 and 7), or HKαS806C + HKβgd (lanes 4 and 8, see asterisks in the injection scheme), or from uninjected oocytes (lanes 1 and 5). Detection used anti-H,Kα antibody HK12.18 (upper panel) or anti-H,Kβ antibody 2G11 (lower panel). One representative Western blot out of at least 3 from different oocyte batches is shown in A and B.

were recorded simultaneously using a Digidata 1322A interface and subsequently analyzed with Clampex 9.2 and Clampfit 9.2 software (Molecular Devices, Sunnyvale, CA).

Analysis of Transient Currents of the Na,K-ATPase. Presteady state currents under high extracellular Na^+/K^+-free conditions were obtained by subtracting the current responses to voltage steps from −40 mV to values between +60 mV and −180 mV (20 mV increments) in the presence of 10 mM ouabain (inhibiting the endogenously as well as the heterologously expressed pump) from currents measured in the presence of 10 μM ouabain (inhibiting only the endogenous Na,K-ATPase). The resulting difference currents were fitted monoexponentially, disregarding the first 3–5 ms after the voltage step to exclude capacitive artifacts. The translocated charge Q was calculated from the integral of the fitted transient currents, and the resulting $Q-V$ curves were approximated by a Boltzmann function: $Q(V) = Q_{max} + (Q_{max} - Q_{min})/(1 + \exp(z_q F / RT(V - V_{0.5})))$ where Q_{min} and Q_{max} are the saturating values of translocated charge, $V_{0.5}$ is the midpoint potential, z_q the fraction of charge displaced through the entire transmembrane field, F the Faraday constant, R the molar gas constant, T the temperature (in K) and V the transmembrane potential. The turnover number of the Na,K-ATPase was calculated by dividing the stationary current (in nA) at 10 mM K^+ and −40 mV by the difference $Q_{min} - Q_{max}$ (in nC) measured on the same oocyte. All experiments were performed at 23–24 °C.

RESULTS

Plasma Membrane Delivery and α-Subunit Stabilization of the Glycosylation-Deficient Mutants. To assess the question whether N-linked glycosylation is necessary for cell surface delivery of the Na,K- or H,K-ATPase, plasma membranes were isolated from injected oocytes and compared to total membrane preparations by Western blotting. Importantly, the glycosylation-deficient variants of both Na,K- and H,K-ATPase were delivered to the plasma membrane (lanes 4 in Figures 2A and 2B, respectively). Regarding the H,K-ATPase wild type β-subunit, the broad region from 60 to 70 kDa detected by the anti-H,K β-antibody (Figure 2 B, lane 3) is characteristic for complex-type oligosaccharides due to considerable variety in number and composition of terminal sugars, giving rise to the heterogeneity of the mature glycosylated H,K-ATPase β-subunit. Likewise, a similar broad band would be expected for the fully glycosylated Na,K β-subunit in the respective plasma membrane fraction, but only a rather weak discrete band is stained by the anti Na,K β-antibody. Since it is also present in all other lanes from Figure 2A, including control preparations from uninjected or only α-subunit cRNA-injected oocytes, it must be mainly attributed to the endogenously expressed *Xenopus laevis* Na,K-ATPase β-subunit. Although the α-subunit is strongly expressed, a substantially more intense band indicating expression of heterologous Na,K-ATPase β-subunit is absent in the corresponding plasma membrane fraction (Figure 2A, lane 3). Notably, the epitope recognized by the M17-P5-F11 antibody is only two amino acids separated from the second glycosylation site N193 (*11*). Obviously, the majority of the various complex-type oligosaccharides attached to this site impairs antibody binding, leading to a low detection efficiency for the glycosylated protein. This interpretation is in agreement with previous studies which have demonstrated a 10-fold stronger antibody binding to this epitope after enzymatic removal of N-linked carbohydrates (*11*). Moreover, this is supported by the intense focused band at 41 kDa observed in the total cellular membrane fraction (Figure 2A, lane 7) prepared from the same oocyte sample as the plasma membrane preparation, which is characteristic for Na,K-ATPase β-subunits carrying high mannose precursor oligosaccharides. Since these are readily detected by the antibody, apparently the terminal sugars added in the very last steps of glycosylation interfere with antibody binding. As these high mannose precursors were reported to remain intracellularly, being unable to reach the plasma membrane until completely glycosylated (*9*) (*10*), this band is exclusively observed in the total cellular

Table 1: Stationary Currents and Turnover Number of Na,K-ATPase α/β Complexes Containing Wild Type or Nonglycosylated β-Subunits[a]

	stationary current (nA)	turnover number (s^{-1})
NaKα/βS62C	255 ± 24	34.2 ± 3.2
NaKα/βS62Cgd	205 ± 19	32.5 ± 2.3

[a] Values are means ± SE of 5–12 oocytes from two different oocyte batches.

membrane fraction. Moreover, its absence in the plasma membrane fraction excludes any contamination of this sample by total cellular membranes.

Analogously, the 50 kDa band uniquely present in the HKαwt/HKβwt total cellular membrane fraction (Figure 2B, lane 7) is characteristic for the H,K-ATPase β-subunit's immature, mannose-rich glycosylation. For the glycosylation-deficient Na,K- and H,K-ATPase mutants, these bands are each shifted to lower molecular weights of about 32–34 kDa for both enzymes, corresponding to the protein core, which is seen in both plasma (Figure 2A and Figure 2B, lane 4) and total membrane fractions (Figure 2A and Figure 2B, lane 8). The band at high molecular weights in the total membrane fraction of glycosylation-deficient H,K-ATPase (Figure 2B, lane 8) could potentially represent aggregates formed between the fully deglycosylated H,K-ATPase β-subunits, which do not dissociate even under denaturating conditions. It has been proposed that core sugars have a global effect on the solubility of newly synthesized proteins that counteracts the tendency to form irreversible aggregates by hydrophobic interactions (*36*).

Notably, the glycosylation-deficient Na,K- and H,K-ATPase β-subunits were able to stabilize their corresponding α-subunit equally well as their glycosylated counterparts, as judged from the amount of the 100 kDa α-subunit protein detected in the plasma membrane fraction (Figure 2A and Figure 2B, compare upper lanes 3 and 4 each). In contrast, when Na,K- or H,K-ATPase α-subunits are expressed without their corresponding β-subunits, the heterologous cRNA is translated into protein, which, however, is not targeted to the plasma membrane, but remains in intracellular (mainly ER) membranes, thus explaining the presence of a 100 kDa band in both lanes 6 and its absence in both lanes 2 in Figure 2A and Figure 2B. Furthermore, the intracellularly retained Na,K-ATPase α-subunit is more susceptible to cellular degradation, as indicated by the bands below 100 kDa also detected by the Na,K α-antibody in the total membrane preparation (Figure 2A, lane 6). This phenomenon has been reported previously (*37*). The results from these control experiments support the notion that the observed plasma membrane stabilization of the α-subunits is indeed brought about by association with the coexpressed glycosylation-deficient β-subunits, rather than by assembly with the endogenously expressed Na,K β-subunit.

Enzyme Activity of Glycosylation-Deficient Mutants. To test whether the enzymes assembled from glycosylation-deficient Na,K- and H,K-ATPase β-subunit mutants are still functional in the plasma membranes of *Xenopus* oocytes, the transport activity was assessed by measuring K^+ activated stationary currents for the electrogenic Na,K-ATPase and by rubidium uptake measurements for the electroneutrally operating H,K-ATPase. Table 1 shows the stationary currents observed under saturating K^+ concentrations. Values are identical within error limits for the glycosylation-deficient and the glycosylation-competent enzyme. Similarly, the turnover number is not influenced by the glycosylation status (see Table 1). Thus, both the amount of functional enzyme on the cell surface and ion pumping activity of the Na,K-ATPase are not affected by the removal of N-linked oligosaccharides from the β-subunit.

As illustrated in Figure 3A, Rb^+ transport activity under saturating extracellular rubidium concentrations is also quite similar when comparing oocytes expressing glycosylated and glycosylation-deficient H,K-ATPase complexes, and is clearly higher than in uninjected oocytes or in cells expressing only H,K-ATPase α-subunits. Specificity of Rb^+ uptake is demonstrated by inhibition with the H,K-ATPase inhibitors SCH28080 (Figure 3A) and omeprazole (data not shown). Furthermore, the apparent constant for half-maximal Rb^+ activation ($K_{0.5}$) derived from Figure 3B (inset) is very similar for glycosylated and glycosylation-defective H,K-ATPase (0.67 ± 0.04 mM versus 0.64 ± 0.04 mM).

E_1P/E_2P Conformational Distribution and Kinetics of E_1P/E_2P Transition of Glycosylation-Deficient Mutants. To investigate whether removal of the huge sugar moiety influences the kinetics of the E_1P/E_2P conformational change, the mutated ATPases were also studied by voltage-clamp fluorometry. TMRM-labeled oocytes expressing the wild type Na,K-ATPase α-subunit together with either the glycosylation-competent βS62C or the glycosylation-deficient βS62Cdg β-subunit were subjected to voltage pulses and the resulting conformation-dependent fluorescence changes (Figure 4A) were analyzed. When a Boltzmann function is fitted to the corresponding $(1 - \Delta F/F)-V$ distributions, the voltage dependence is very similar for glycosylated and glycosylation-deficient enzymes (Figure 4C), thus yielding identical fit parameters within error limits (Table 2). As illustrated in Figure 4D, these $(1 - \Delta F/F)-V$ curves are strictly correlated to the voltage-dependent distribution of charge movement ($Q-V$ curves, see Table 2 for Boltzmann parameters), which was determined from transient currents recorded in parallel (Figure 4F, inset). Time constants for the voltage-dependent E_1P/E_2P transition resulting from monoexponential fits of the fluorescence signals are presented in Figure 4D for βS62C and the glycosylation-deficient βS62Cgd variant. Likewise, Figure 4E shows the reciprocal time constants of the simultaneously recorded transient currents, which are about 4 times larger than those from fluorescence changes at hyperpolarizing potentials, as observed previously (*27*). Since both time constants determined for the glycosylation-deficient mutant are comparable to the fully glycosylated enzyme, the kinetics of the voltage-dependent E_1P/E_2P transition seems unaffected by the bulky sugars on the β-subunit.

To address the same question for the even more heavily glycosylated H,K-ATPase, the wild type and glycosylation-deficient β-isoforms were coexpressed together with the aforementioned S806C variant of the H,K-ATPase α-subunit. Application of the same voltage steps as in the protocol used for the Na,K-ATPase (Figure 4A, inset) to TMRM-labeled oocytes expressing these constructs resulted under K^+-free conditions in fluorescence changes as presented in Figure 5A. Provided that Na,K- and H,K-ATPase reaction mechanisms during voltage pulse experiments in the absence of extracellular K^+ are similar, one would also expect a voltage dependence of fluorescence amplitudes ($(1 - \Delta F/F)-V$ curve) according to a Boltzmann function, implying that H,K-

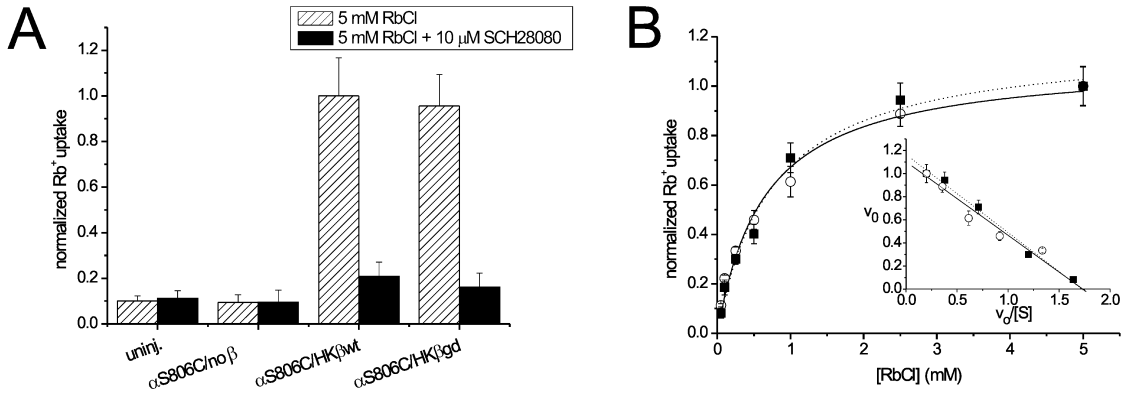

FIGURE 3: Rb^+ uptake into oocytes by H,K-ATPase with wild type or glycosylation-deficient β-subunits. (A) H,K-ATPase-mediated Rb^+ uptake at 5 mM RbCl in the absence (hatched bars) or presence (black bars) of 10 μM SCH28080. Results from uninjected control oocytes or oocytes injected with the following cRNAs are shown: HKαS806C only, HKαS806C + HKβwt, or HKαS806C + HKβgd. Data were normalized to αS806C/βwt H,K-ATPase Rb^+ uptake in the absence of SCH28080, corresponding to 14.0, 18.6 and 19.7 pmol/oocyte/min. (B) Michaelis–Menten plot for Rb^+ uptake by H,K-ATPase. Inset: Eadie−Hofstee plot. Oocytes were injected with HKαS806C- and HKβwt-cRNA (■) or with HKαS806C- and HKβgd-cRNA (○), respectively. Data were normalized to Rb^+ uptake at 5 mM RbCl, corresponding to 18.5 and 9.9 pmol/oocyte/min for HKαS806C/βwt; 14.1, 20.7 and 18.7 pmol/oocyte/min for HKαS806C/βgd. Rb^+ uptake was measured on individual cells by atomic absorption spectroscopy (see Experimental Procedures). Data are means ± SE, n = 8–10 oocytes from 2 or 3 experiments.

ATPase can be shifted saturatingly between E_1P and E_2P states. Thus, the almost linear distribution observed between the −200 mV and +60 mV argues for a reduced voltage sensitivity of the H,K-ATPase compared to Na,K-ATPase. Although fits of a Boltzmann function to $(1 - \Delta F/F)-V$ curves are less well defined, since saturation of fluorescence amplitudes cannot be reached within the experimentally accessible voltage range, consistent fit results were obtained on many different cells. The resulting value for the equivalent charge z_q of ∼0.3 for the gastric H,K-ATPase can be considered as an upper limit, since fits of a Boltzmann function would yield even lower z_q values, if the approximately linear progression of the $Q-V$ curve would extend over an even larger voltage range. As shown in Figure 5B, there are no discernible differences between the voltage dependence of fluorescence amplitudes for the wild type and the glycosylation-deficient H,K-ATPase β mutant when coexpressed with HKαS806C, thus resulting in distributions with similar Boltzmann parameters (see Table 2). Likewise, the reciprocal time constants from monoexponential fitting of the fluorescence changes (Figure 5C) are not significantly different for the glycosylation-deficient and glycosylated H,K-ATPases. Notably, however, they are by a factor of about 5 smaller compared to those of the Na,K-ATPase (Figure 4D) and their voltage dependence is also substantially weaker. This fits well with the aforementioned reduced voltage dependence of $(1 - \Delta F/F)-V$ curves, reflected by the much lower z_q value (∼0.30 versus ∼0.75 for the Na,K-ATPase, see Table 2). Together, these two phenomena may explain why all our attempts failed to measure transient currents on H,K-ATPase-expressing oocytes using the two-electrode voltage-clamp or the giant excised patch-clamp technique (unpublished observations). Since the electrogenicity of both the H^+-carrying (*38*) and the K^+-transporting limb (*39*) of the H,K-ATPase catalytic cycle has been demonstrated, such currents probably exist, but the at least 2 to 3 times lower amount of charge transported with approximately 5-fold lower reciprocal time constants would result in substantially smaller current amplitudes compared to the sodium pump, which are difficult to resolve in voltage-jump experiments.

DISCUSSION

In this study, the role of N-linked carbohydrates in the function of Na,K- and H,K-ATPase was examined in *Xenopus* oocytes. The results were surprisingly similar for both investigated enzymes, with no discernible differences between the glycosylation-defective variants and the fully glycosylated enzymes. Plasma membrane delivery, association with the α-subunit and ion transport activities were virtually unaffected by the lack of N-linked glycans. Moreover, apparent ion affinities were unaltered and even intricate details of the catalytic cycle, such as the voltage-dependent distribution between E_1 and E_2 states, as well as the kinetics of the voltage-dependent E_1P/E_2P transition were essentially the same for glycosylation-deficient Na,K- and H,K-ATPase β-variants when compared to their glycosylated counterparts. While this is in agreement with previous glycosylation studies on Na,K ATPase (*9–13*), similar investigations on the gastric H,K-ATPase using other expression systems had resulted in very dissimilar observations:

Whereas α/β coassembly tested by immunoprecipitation was unaffected for fully deglycosylated H,K-ATPase β-subunits in tunicamycin treated Sf9 cells (*8*) and single-site glycosylation-defective variants expessed in HEK293 cells, the amount of coprecipitated α-subunit was substantially lower when more than four glycosylation sites were deleted and was successively reduced with each deleted site in the mammalian expression system (*6*). For the Na,K-ATPase expressed in *Xenopus* oocytes, slightly lower amounts of α-subunit were coprecipitated with a completely glycosylation-defective mutant than with the glycosylated wild type β-subunit (*12*), also indicating a destabilization of the α/β interaction. Yet, the findings from the present study do not hint at a destabilizing effect on the α/β coassembly caused by the lack of carbohydrates for both Na,K- and H,K-ATPase. Although we did not use immunoprecipitation to

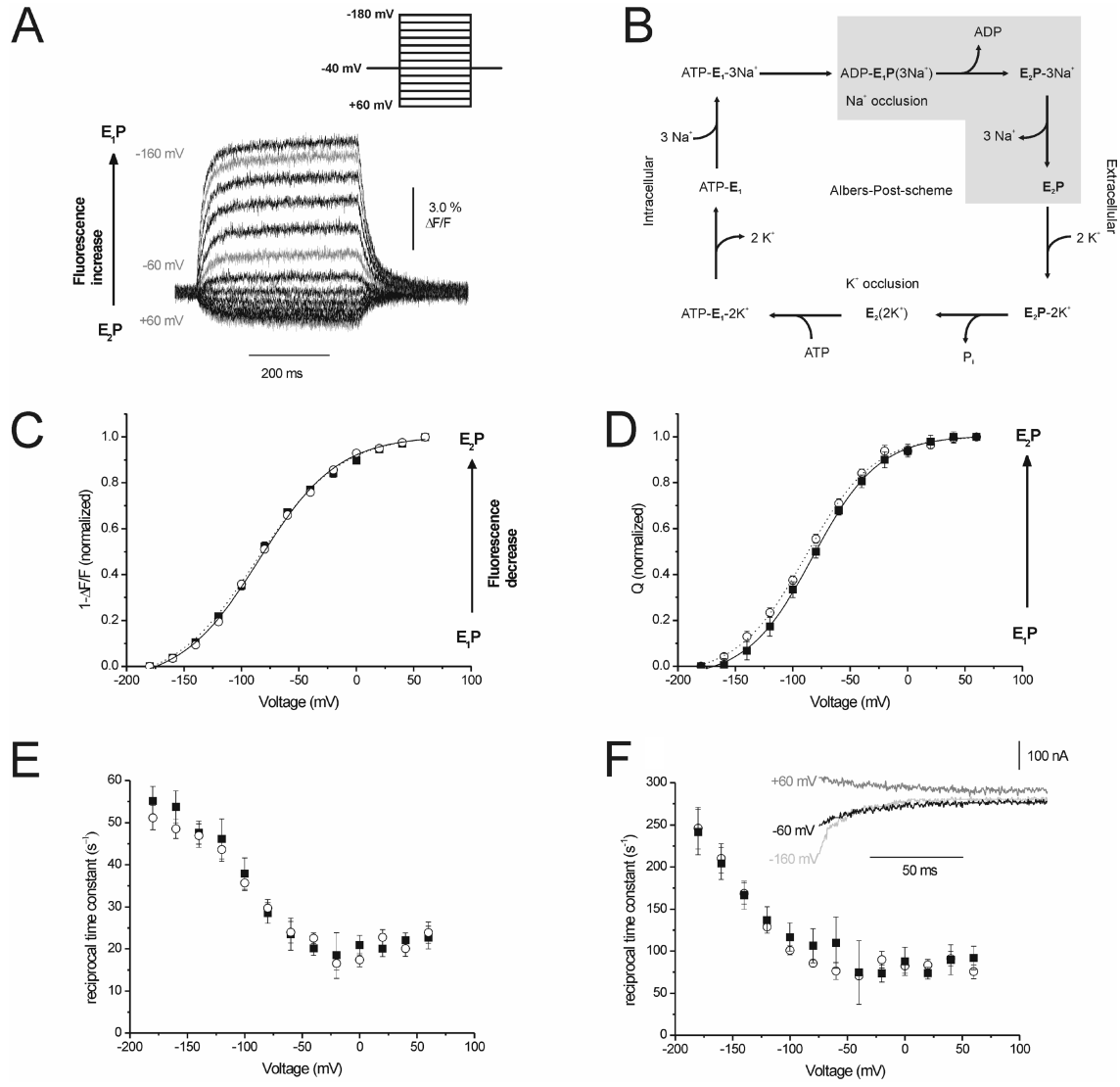

FIGURE 4: Voltage dependence of E_1P/E_2P distribution and kinetics of E_1P/E_2P transitions of Na,K-ATPase enzymes with glycosylated or nonglycosylated β-subunits. (A) Fluorescence signals of the site-specifically labeled Na,K-ATPase in response to voltage pulses (see inset) from −40 mV to values between +60 mV and −180 mV in 20 mV steps under extracellularly high Na^+/K^+-free conditions are shown. Data originated from an oocyte coexpressing NaKαwt + NaKβS62C. Traces for voltage jumps to −160 mV, −60 mV and +60 mV are shown in gray. (B) Albers−Post scheme for the Na,K-ATPase reaction cycle. The Na,K-ATPase assumes two distinct conformational states: E_1, with binding sites facing the cytosol, and E_2, with binding sites open to the extracellular space. The main electrogenic event was assigned to Na^+ transport steps which are kinetically coupled to the E_1P–E_2P transition (underlaid in gray). (C, D) Voltage dependence of fluorescence amplitudes $1 - \Delta F/F$ (C) and transient charge movements Q (D) for Na,K-ATPase complexes containing glycosylated NaKβS62C (■) or nonglycosylated NaKβS62Cgd (○) β-subunits (conditions as in A). Data are means ± SE of 10–24 oocytes, normalized to saturating values at −180 mV after subtracting the values for +60 mV. A curve corresponding to the fit of a Boltzmann function is superimposed. (E, F) Reciprocal time constants of voltage jump-induced fluorescence changes (E) and transient currents (F) for Na,K-ATPase complexes containing glycosylated NaKβS62C (○) β-subunits (conditions as in A). Data are means ± SE of 8–15 oocytes. (F, inset) Transient currents recorded from an oocyte coexpressing NaKαwt + NaKβS62C for voltage jumps from −40 mV to −160 mV, −60 mV and +60 mV, obtained as ouabain-sensitive difference currents (conditions as in A) recorded in parallel to fluorescence signals (see Experimental Procedures).

Table 2: Parameters from Fits of a Boltzmann Function to $Q-V$ Distributions of Na,K-ATPase (Figure 4D) and $(1 - \Delta F/F)-V$ Distributions of Na,K-ATPase or H,K-ATPase (Figure 4C and Figure 5B)

	$(1 - \Delta F)/V$ curves		Q/V curves	
	$V_{0.5}$ (mV)	z_q	$V_{0.5}$(mV)	z_q
NaKαwt/βS62C	−86.9 ± 2.9	0.71 ± 0.02	−88.7 ± 1.5	0.87 ±0.04
NaKαwt/βS62Cgd	−84.4 ± 2.4	0.75 ± 0.03	−82.6 ± 0.9	0.89 ±0.03
HKαS806C/βwt	−19.6 ± 5.4	0.26 ± 0.02		
HKαS806C/βgd	−18.9 ± 4.6	0.27 ± 0.02		

directly probe interaction of the glycosylation-deficient β-subunits with their corresponding α-subunits, we drew our conclusions (i) from quantifying the amount of coexpressed α-subunit delivered to the plasma membrane as judged by immunoblotting of the plasma membrane protein fraction and (ii) by measuring the ion transport activity of ATPase

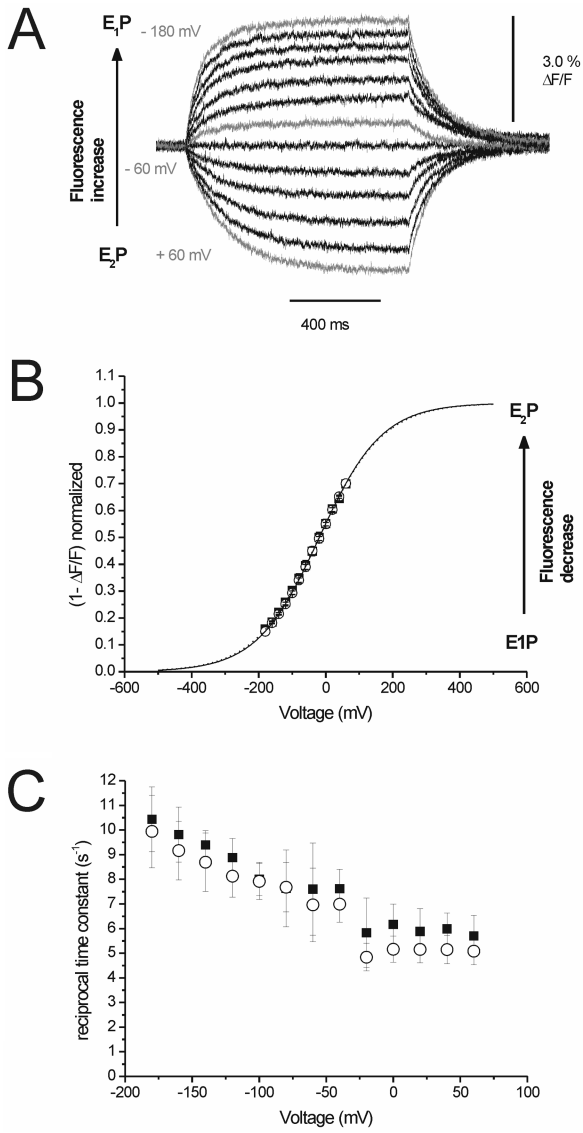

FIGURE 5: Analysis of the E_1P/E_2P distribution and kinetics of H,K-ATPase containing wild type or nonglycosylated β-subunits by voltage-clamp fluorometry. (A) Voltage pulse-induced fluorescence responses of the site-specific labeled H,K-ATPase under K^+-free conditions (pH 7.4). Recordings originated from an oocyte coexpressing HKαS806C + HKβwt. (B) Voltage dependence of fluorescence amplitudes ($1 - \Delta F/F$) under K^+-free conditions for H,K-ATPase construct HKαS806C containing glycosylated HKβwt (■) or nonglycosylated HKβgd (○) β-subunits. Data are means ± SE of 10–13 oocytes. A curve resulting from a fit of a Boltzmann function is superimposed. The fluorescence amplitudes $1 - \Delta F/F$ were normalized to saturation values from the fits. (C) Reciprocal time constants of voltage jump-induced fluorescence changes under K^+-free conditions for the H,K-ATPase αS806C construct containing glycosylated HKβwt (■) or nonglycosylated HKβgd (○) β-subunits. Data are means ± SD from 9−11 oocytes.

molecules present in the plasma membrane of intact oocytes. We think this is an equally legitimate approach, since according to all previously published data, α/β coassembly is an essential prerequisite for plasma membrane delivery of the α-subunit and enzymatic activity of Na,K-ATPase (*2, 40*) and H,K-ATPase (*3*) holoenzymes. In addition to α/β association, also the plasma membrane delivery of the H,K-ATPase was impaired for glycosylation-defective mutants in previous studies using confocal microscopy or immunofluorescence. Whereas single or double glycosylation site-deleted H,K-ATPase β-subunits still supported some α-subunit cell surface expression, deletion of all glycosylation sites prevented plasma membrane delivery in COS-1 cells (*6*). In HEK293 cells however, every single-site deletion already abolished plasma membrane delivery, except for the deletion of the nonconserved glycosylation site Asn103 (*7*). In the Sf9 expression system, the situation is even more complicated due to the fact that even the normally glycosylated, catalytically active wild type holoenzyme was not found in the plasma membrane of insect cells, but had to be retrieved from intracellular membrane structures. However, the fully glycosylated wild type β-subunit was partly targeted to the plasma membrane, even when the α-subunit was not coexpressed, whereas plasma membrane delivery was not observed after a complete removal of N-linked sugars by tunicamycin treatment of Sf9 cells (*8*). Therefore, the authors concluded that plasma membrane delivery of the β-subunit depends on N-linked glycosylation. Eventually, ATPase activity was completely lost both for tunicamycin-treated, H,K-ATPase-transfected insect cells (*8*) and for a fully N-glycosylation-deficient H,K-ATPase variant expressed in HEK293 cells according to Asano and co-workers (*6*). Single or double site-deleted mutants still exhibited normal activity in HEK293 cells, but each additional deletion resulted in decreased activity (*6*). Similarly, Vagin and co-workers reported unaltered enzymatic properties and SCH28080 inhibition kinetics for every single- and some double-deletion variant stably expressed in HEK cells (*7*).

These observations disagree with our results that rubidium transport activity of the glycosylation-defective variant is not different from glycosylated H,K-ATPase in *Xenopus* oocytes. In our opinion, this expression system has several advantages: Stationary currents of the Na,K-ATPase and rubidium uptake of the H,K-ATPase were measured on intact plasma membranes from living oocytes, whereas in the other expression systems enzymatic activity was determined in crude membrane fractions, which do not differentiate between plasma membrane and intracellular membranes. For the latter studies it is therefore more likely that the loss of activity and potentially also the impaired α/β coassembly observed for completely deglycosylated H,K-ATPase occurred as a consequence of preparational procedures and would possibly not be observed when determined on intact cells or on pure plasma membrane protein fractions. The lack of sugar moieties seems to render the enzyme more susceptible to inactivation than the glycosylated wild type isoform during preparational procedures, which apparently does not happen as long as the enzyme is stabilized in a native plasma membrane environment. Results from purification studies on Na,K-ATPase isolated from *Pichia pastoris* support this idea, since it was reported that enzymatic removal of all N-linked carbohydrates from isolated Na,K-ATPase molecules reduced their activity, especially when facing certain ionic conditions and lipid compositions. The presence of some particular phospholipids on the other hand conserved enzymatic activity of the deglycosylated enzyme (*41*). In this context it is interesting to note that activity measurements in most studies on glycosylation-defective Na,K-ATPase mutants were also carried out in living cells, mainly in oocytes (*9, 12*). H,K-ATPase activity might even be more sensitive to preparational impairment than that of Na,K-ATPase, considering its high sensitivity to inactivation by detergents (*8*). An even

more likely explanation for the discrepancies found between glycosylation-deficient H,K-ATPase variants expressed in oocytes and the other two mentioned expression systems might be that the observed differences are temperature-related. It was shown that glycosylation increases the thermal stability of proteins, resulting from largely entropic rather than enthalpic effects (*42*). This might also explain why the α/β interaction of a glycosylation-defective variant is only disrupted in mammalian cells cultured at 37 °C, but not in oocytes or Sf9 cells, which are incubated at 17 and 27 °C, respectively. Minor folding impairments potentially occurring already at 27 °C might not affect α/β coassembly but still abolish enzymatic activity, possibly explaining the loss of H,K-ATPase activity reported for the Sf9 expression system.

Although the oocyte system may be regarded as physiologically less relevant, the observation of unimpaired H,K-ATPase activity of glycosylation-deficient mutants in the current study is valuable, because the role of N-linked sugars on enzyme function can be clarified. Our findings of a completely unaffected surface delivery of glycosylation-deleted mutants are rather incompatible with the idea that the carbohydrates are essential for correct folding and intersubunit association for both Na,K- and H,K-ATPase. However, they are not contradicting the role of the N-glycans for basolateral sorting reported for Na,K-ATPase complexes containing β_1-subunits (*18*) versus apical sorting for Na,K-ATPase holoenzymes comprising β_2-subunits (*17*), and H,K-ATPase with fully glycosylated H,K β-subunits (*20*). In the nonpolarized oocyte, such targeting signals may not be recognized. For instance, a Y20A mutation in the basolateral sorting/endocytosis signal sequence FRXY present in the H,K-ATPase β-subunit was shown to enhance apical targeting of the H,K-ATPase *in vivo* (*43, 44*) and in polarized MDCK, but not LLC-PK cells (*45*). In contrast, immunoblotting of isolated plasma membranes or Rb^+ uptake measurements did not reveal any differences in the amount of active H,K-ATPase in the plasma membrane, when *Xenopus* oocytes expressing the α-subunit together with the same H,K β-subunit Y20A or the wild type β-subunit were compared (unpublished observations).

Apart from their importance as apical sorting signals in polarized cells, the N-linked carbohydrates of the gastric H,K-ATPase β-subunits may have a protective role *in situ*. It was shown that the composition of terminal sugars of the H,K-ATPase oligosaccharides in parietal cells is quite different from other glycosylated proteins (e.g., absence of sialic acid *23, 46*) and possibly designed to resist hydrolysis of the carbohydrate chains in the acidic stomach lumen. This in turn raises the question, why the integrity of the carbohydrates is important for the gastric H,K-ATPase, once delivered to the plasma membrane. Interestingly, it was shown that the removal of N- or O-linked carbohydrates destabilizes a variety of proteins and tends to make them more susceptible to aggregation, especially at low pH (*47, 48*). Moreover, results from several studies indicate that the removal of oligosaccharides renders the H,K-ATPase more sensitive toward proteolytic digestion by various enzymes including pepsin (*21, 22*). Notably, a similar protective role of glycosylation has been demonstrated for other gastrointestinally active enzymes (*49, 50*).

In summary, the results from the current study on *Xenopus* oocytes favor the idea that in analogy to the Na,K-ATPase, glycosylation of the H,K-ATPase is dispensable for protein stability and enzyme function itself, but is rather important for other functions primarily relevant in native tissues.

ACKNOWLEDGMENT

We thank Janna Lustig for assistance in molecular biology and Robert Dempski for fruitful discussions.

SUPPORTING INFORMATION AVAILABLE

Figure depicting Rb^+ transport of the H,K-ATPase wild type and mutant αS806C. This material is available free of charge via the Internet at http://pubs.acs.org.

REFERENCES

1. Axelsen, K. B., and Palmgren, M. G. (1998) Evolution of substrate specificities in the P-type ATPase superfamily. *J. Mol. Evol. 46*, 84–101.
2. McDonough, A. A., Geering, K., and Farley, R. A. (1990) The sodium pump needs its beta subunit. *FASEB J. 4*, 1598–1605.
3. Gottardi, C. J., and Caplan, M. J. (1993) Molecular requirements for the cell-surface expression of multisubunit ion-transporting ATPases. Identification of protein domains that participate in Na,K-ATPase and H,K-ATPase subunit assembly. *J. Biol. Chem. 268*, 14342–14347.
4. Altendorf, K., and Epstein, W. (1994) Kdp-ATPase of *Escherichia coli*. *Cell. Physiol. Biochem. 4*, 160–168.
5. Lutsenko, S., and Kaplan, J. H. (1995) Organization of P-type ATPases: significance of structural diversity. *Biochemistry 34*, 15607–15613.
6. Asano, S., Kawada, K., Kimura, T., Grishin, A. V., Caplan, M. J., and Takeguchi, N. (2000) The roles of carbohydrate chains of the beta-subunit on the functional expression of gastric H^+,K^+-ATPase. *J. Biol. Chem. 275*, 8324–8330.
7. Vagin, O., Denevich, S., and Sachs, G. (2003) Plasma membrane delivery of the gastric H,K-ATPase: the role of beta-subunit glycosylation. *Am. J. Physiol.: Cell Physiol. 285*, C968–976.
8. Klaassen, C. H., Fransen, J. A., Swarts, H. G., and De Pont, J. J. (1997) Glycosylation is essential for biosynthesis of functional gastric H^+,K^+-ATPase in insect cells. *Biochem. J. 321* (Pt 2), 419–424.
9. Takeda, K., Noguchi, S., Sugino, A., and Kawamura, M. (1988) Functional activity of oligosaccharide-deficient (Na,K)ATPase expressed in *Xenopus* oocytes. *FEBS Lett. 238*, 201–204.
10. Tamkun, M. M., and Fambrough, D. M. (1986) The Na^+,K^+-ATPase of chick sensory neurons. Studies on biosynthesis and intracellular transport. *J. Biol. Chem. 261*, 1009–1019.
11. Sun, Y., and Ball, W. J. (1994) Identification of antigenic sites on the Na^+/K^+-ATPase beta-subunit: their sequences and the effects of thiol reduction upon their structure. *Biochim. Biophys. Acta 1207*, 236–248.
12. Beggah, A. T., Jaunin, P., and Geering, K. (1997) Role of glycosylation and disulfide bond formation in the beta subunit in the folding and functional expression of Na,K-ATPase. *J. Biol. Chem. 272*, 10318–10326.
13. Zamofing, D., Rossier, B. C., and Geering, K. (1989) Inhibition of N-glycosylation affects transepithelial Na^+ but not Na^+-K^+-ATPase transport. *Am. J. Physiol. 256*, C958–966.
14. Kitamura, N., Ikekita, M., Sato, T., Akimoto, Y., Hatanaka, Y., Kawakami, H., Inomata, M., and Furukawa, K. (2005) Mouse Na^+/K^+-ATPase beta1-subunit has a K^+-dependent cell adhesion activity for beta-GlcNAc-terminating glycans. *Proc. Natl. Acad. Sci. U.S.A. 102*, 2796–2801.
15. Vagin, O., Tokhtaeva, E., and Sachs, G. (2006) The role of the beta1 subunit of the Na,K-ATPase and its glycosylation in cell-cell adhesion. *J. Biol. Chem. 281*, 39573–39587.
16. Heller, M., von der Ohe, M., Kleene, R., Mohajeri, M. H., and Schachner, M. (2003) The immunoglobulin-superfamily molecule basigin is a binding protein for oligomannosidic carbohydrates: an anti-idiotypic approach. *J. Neurochem. 84*, 557–565.
17. Vagin, O., Turdikulova, S., and Sachs, G. (2005) Recombinant addition of N-glycosylation sites to the basolateral Na,K-ATPase beta1 subunit results in its clustering in caveolae and apical sorting in HGT-1 cells. *J. Biol. Chem. 280*, 43159–43167.

18. Lian, W. N., Wu, T. W., Dao, R. L., Chen, Y. J., and Lin, C. H. (2006) Deglycosylation of Na^+/K^+-ATPase causes the basolateral protein to undergo apical targeting in polarized hepatic cells. *J. Cell Sci. 119*, 11–22.
19. Vagin, O., Turdikulova, S., and Tokhtaeva, E. (2007) Polarized membrane distribution of potassium-dependent ion pumps in epithelial cells: Different roles of the N-glycans of their beta subunits. *Cell Biochem. Biophys. 47*, 376–391.
20. Vagin, O., Turdikulova, S., and Sachs, G. (2004) The H,K-ATPase beta subunit as a model to study the role of N-glycosylation in membrane trafficking and apical sorting. *J. Biol. Chem. 279*, 39026–39034.
21. Thangarajah, H., Wong, A., Chow, D. C., Crothers, J. M., Jr., and Forte, J. G. (2002) Gastric H-K-ATPase and acid-resistant surface proteins. *Am. J. Physiol.: Gastrointest, Liver Physiol, 282*, G953–G961.
22. Crothers, J. M., Jr., Asano, S., Kimura, T., Yoshida, A., Wong, A., Kang, J. W., and Forte, J. G. (2004) Contribution of oligosaccharides to protection of the H,K-ATPase beta-subunit against trypsinolysis. *Electrophoresis 25*, 2586–2592.
23. Tyagarajan, K., Townsend, R. R., and Forte, J. G. (1996) The Beta-subunit of the rabbit H,K-ATPase:a glycoprotein with all terminal lactosamine units capped with alpha-linked galactose residues. *Biochemistry 35*, 3238–3246.
24. Hu, Y. K., and Kaplan, J. H. (2000) Site-directed chemical labeling of extracellular loops in a membrane protein-The topology of the Na,K-ATPase alpha-subunit. *J. Biol. Chem. 275*, 19185–19191.
25. Price, E. M., and Lingrel, J. B. (1988) Structure-function-relationships in the Na,K-ATPase alpha-subunit: Site directed mutagenesis of glutamine-111 and asparagine-122 to aspartic acid generates a ouabain-resistant enzyme. *Biochemistry 27*, 8400–8408.
26. Lorenz, C., Pusch, M., and Jentsch, T. J. (1996) Heteromultimeric CLC chloride channels with novel properties. *Proc. Natl. Acad. Sci. U.S.A. 92*, 13362–13366.
27. Dempski, R. E., Friedrich, T., and Bamberg, E. (2005) The Beta Subunit of the Na^+/K^+-ATPase Follows the Conformational State of the Holoenzyme. *J. Gen. Physiol. 125*, 505–520.
28. Geibel, S., Kaplan, J. H., Bamberg, E., and Friedrich, T. (2003) Conformational dynamics of the Na^+/K^+-ATPase probed by voltage clamp fluorometry. *Proc. Natl. Acad. Sci. U.S.A. 100*, 964–969.
29. Geibel, S., Zimmermann, D., Zifarelli, G., Becker, A., Koenderink, J. B., Hu, Y. K., Kaplan, J. H., Friedrich, T., and Bamberg, E. (2003) Conformational dynamics of Na^+/K^+- and H^+/K^+-ATPase probed by voltage clamp fluorometry. *Ann. N.Y. Acad. Sci. 986*, 31–38.
30. Kamsteeg, E. J., and Deen, P. M. (2000) Importance of aquaporin-2 expression levels in genotype -phenotype studies in nephrogenic diabetes insipidus. *Am. J. Physiol.: Renal Physiol. 279*, F778–784.
31. Laemmli, U. K. (1970) Cleavage of structural proteins during the assembly of the head of bacteriophage T4. *Nature 227*, 680–685.
32. Koenderink, J. B., Geibel, S., Grabsch, E., De Pont, J. J., Bamberg, E., and Friedrich, T. (2003) Electrophysiological analysis of the mutated Na,K-ATPase cation binding pocket. *J. Biol. Chem. 278*, 51213–51222.
33. Ball, W. J., Jr., Abbott, A., Sun, Y., and Malik, B. (1992) Monoclonal antibodies and the identification of functional regions of the Na^+,K^+-ATPase. *Ann. N.Y. Acad. Sci. 671*, 436–439.
34. Chow, D. C., and Forte, J. G. (1993) Characterization of the beta-subunit of the H^+-K^+-ATPase using an inhibitory monoclonal antibody. *Am. J. Physiol. 265*, C1562–C1570.
35. Rakowski, R. F. (1993) Charge movement by the Na/K pump in *Xenopus* oocytes. *J. Gen. Physiol. 101*, 117–144.
36. Marquardt, T., and Helenius, A. (1992) Misfolding and aggregation of newly synthesized proteins in the endoplasmic reticulum. *J. Cell Biol. 117*, 505–513.
37. Geering, K., Theulaz, I., Verrey, F., Hauptle, M. T., and Rossier, B. C. (1989) A role for the beta-subunit in the expression of functional Na^+-K^+-ATPase in *Xenopus* oocytes. *Am. J. Physiol. 257*, C851–858.
38. van der Hijden, H. T., Grell, E., de Pont, J. J., and Bamberg, E. (1990) Demonstration of the electrogenicity of proton translocation during the phosphorylation step in gastric H^+,K^+-ATPase. *J. Membr. Biol. 114*, 245–256.
39. Lorentzon, P., Sachs, G., and Wallmark, B. (1988) Inhibitory effects of cations on the gastric H^+, K^+ -ATPase. A potential-sensitive step in the K^+ limb of the pump cycle. *J. Biol. Chem. 263*, 10705–10710.
40. Ackermann, U., and Geering, K. (1990) Mutual dependence of Na,K-ATPase alpha- and beta-subunits for correct posttranslational processing and intracellular transport. *FEBS Lett. 269*, 105–108.
41. Cohen, E., Goldshleger, R., Shainskaya, A., Tal, D. M., Ebel, C., le Maire, M., and Karlish, S. J. (2005) Purification of Na^+,K^+-ATPase expressed in *Pichia pastoris* reveals an essential role of phospholipid-protein interactions. *J. Biol. Chem. 280*, 16610–16618.
42. DeKoster, G. T., and Robertson, A. D. (1997) Thermodynamics of unfolding for Kazal-type serine protease inhibitors: entropic stabilization of ovomucoid first domain by glycosylation. *Biochemistry 36*, 2323–2331.
43. Courtois-Coutry, N., Roush, D., Rajendran, V., McCarthy, J. B., Geibel, J., Kashgarian, M., and Caplan, M. J. (1997) A tyrosine-based signal targets H/K-ATPase to a regulated compartment and is required for the cessation of gastric acid secretion. *Cell 90*, 501–510.
44. Wang, T., Courtois-Coutry, N., Giebisch, G., and Caplan, M. J. (1998) A tyrosine-based signal regulates H-K-ATPase-mediated potassium reabsorption in the kidney. *Am. J. Physiol. 275*, F818–826.
45. Roush, D. L., Gottardi, C. J., Naim, H. Y., Roth, M. G., and Caplan, M. J. (1998) Tyrosine-based membrane protein sorting signals are differentially interpreted by polarized Madin-Darby canine kidney and LLC-PK1 epithelial cells. *J. Biol. Chem. 273*, 26862–26869.
46. Beesley, R. C., and Forte, J. G. (1973) Glycoproteins and glycolipids of oxyntic cell microsomes. I. Glycoproteins: carbohydrate composition, analytical and preparative fractionation. *Biochim. Biophys. Acta 307*, 372–385.
47. Wang, C., Eufemi, M., Turano, C., and Giartosio, A. (1996) Influence of the carbohydrate moiety on the stability of glycoproteins. *Biochemistry 35*, 7299–7307.
48. Imperiali, B., and O'Connor, S. E. (1999) Effect of N-linked glycosylation on glycopeptide and glycoprotein structure. *Curr. Opin. Chem. Biol. 3*, 643–649.
49. Rudd, P. M., Joao, H. C., Coghill, E., Fiten, P., Saunders, M. R., Opdenakker, G., and Dwek, R. A. (1994) Glycoforms modify the dynamic stability and functional activity of an enzyme. *Biochemistry 33*, 17–22.
50. Loomes, K. M., Senior, H. E., West, P. M., and Roberton, A. M. (1999) Functional protective role for mucin glycosylated repetitive domains. *Eur. J. Biochem. 266*, 105–111.

BI800092K